Armenian Journal of Physics, 2016, vol. 9, issue 2, pp. 138-146

Dielectric Characteristics of $Pt/Ba_xSr_{1-x}TiO_3/Pt$ Thin Film Structure under the Electron Beam Irradiation

V.V.Buniatyan[1,*], V.M.Tsakanov[2], N.W. Martirosyan[1,2], G.S. Melikyan[1], H.R. Dashtoyan[1]

[1] *National Polytechnic University of Armenia, 0009, Teryan 105, Yerevan, Armenia*
[2] *CANDLE Synchrotron Research Institute, 0040, Yerevan, Armenia*

[*]E-mail:vbuniat@seua.am

Received 25 March 2016

Abstract. The dielectric properties of $aBa_{0.25}Sr_{0.75}TiO_3$films with Pt interdigitated electrodes fabricated by pulsed laser deposition technique and examined under the low-energy electron beam irradiation. The structures were characterized by means of dielectric permittivity,ε-f, C-f, tgδ-f dependencies before and after irradiation over frequency range from 100 Hz to 1 MHz. Irradiations have been carried out in AREAL (Advanced Research Electron Accelerator Laboratory). The energy of electrons has been 4 MeV, bunch charge 10-200 pC, repetition rate 1-50 Hz. It was found that the dielectric permittivity and loss tangent, in general, are shifted to the more low frequency range and decreased after electron beam irradiation.

Keywords: electron beam, irradiation, perovskite-oxide film, interdigitated electrode

1. Introduction

Current interest in perovskite and perovskite-related oxometallates is based on a wide spectrum of their electrical properties, which originates from insulating materials, ionic and/or metallic conductors, p-and n-type-semiconductors to superconductors. The perovskite oxides $A_{1-x}A_x'BO_{3-b}$ have been used in many applications due to their large nonlinear optical coefficients, large dielectric constants, thermal stability and higher catalytic properties. These include high density DRAMs, non-volatile FeRAMs, ferroelectric FETs, SOFCs, voltage-tunable capacitors, microwave electronic components that can work especially at GHz or even THz frequencies, microdevices with pyroelectric and piezoelectric microsensors and actuators, etc. [1-4]. Moreover, perovskite oxides have aroused increasing attention as catalytically active multifunctional materials in the field of (bio-)chemical sensors. Some of such virgin application frontiers for perovskite oxides of different compositions include, for instance, pH sensing [5-9], hydrogen peroxide [10-11] and hydrocarbon detection [12]. One of the most popular and intensively studied multifunctional perovskite-oxide materials is barium strontium titanate [1-3]. In previous experiments, the BST films have been applied for the detection of humidity [13], hydrogen [14] and ammonia gas [15] etc.

Nowadays, there has been an increasing need towards the integration of ferroelectric thin films with the semiconductor technology and the scaling down of device size. The ferroelectric thin films used in the (bio-)chemical sensors, electronic devices, which can find application in the radiation environments such as space, nuclear reactors and nuclear waste containers, will be exposed to constant ionizing radiation and will suffer changes in their performance. Some of these applications require the BST (PZT) based devices to operate in radiation fields where they will be exposed to a high flux of energetic, heavy and light, charged and uncharged particles.

On the other hand it is well known, that radiation effects comprise the variety of microscopic and macroscopic material property changes upon exposure to ionizing radiation. There is a wide range of radiation damage phenomena shared by many types of solids. Some phenomena, however, are unique to a particular solid and depend on its structure, composition, physical dimensions, etc. As a

convenience, radiation effects are frequently broken up into two categories: displacement effects and ionization effects [16-19]. Displacement effects pertain to those properties tied to the arrangement of atoms within a structure, while ionization effects relate to the re-distribution of electrons within the solid. It is well known that irradiation with low energy (< 10 MeV) electron mainly causes point pair defects in crystals. In the case of high electron beam pulse intensity one can expect cluster defects or disordered region formation [19].

The aim of this work is to fabricate a chip sensor based on (Ba,Sr)TiO_3 films with Pt interdigitated electrodes and examined the effect of low energy pulsed electron beam irradiation on dielectric and ferroelectric properties of these thin films. The sensors were characterized by means of dielectric permittivity, *ε-f, C-f, tgδ-f* dependencies before and after irradiation over frequency range from 100 Hz to 1 MHz.

2. Fabrication of the nanostructure (sensor) chips

Planar interdigital electrodes (IDE, with Pt electrodes) sensor were fabricated in Aachen University of Applied Sciences, Institute Nano-and Biosystems, Germany, using the targets of BST prepared in NPUA by means of conventional silicon and thin-film technologies (Fig.1). Initially, a 440 nm SiO_2 layer was grown by thermal wet oxidation on a silicon substrate (p-Si, $\rho = 1000\ \Omega$cm, Topsil Semiconductor Materials, Denmark). A thick SiO_2 layer has been used in order to reduce the influence of the parasitic capacitance of the SiO_2 and the Si resistance on the sensor chip. In the next step, a photolithography process was performed to define a trench area for burying the metal electrodes. To achieve a planar sensor surface, shallow trenches with a depth of ~175 nm were obtained by etching the SiO_2 with hydrofluoric acid. Then, a thin layer of ~10 nm Ti as adhesion layer and ~165 nm Pt as electrode material were deposited by means of electron-beam followed by a lift-off-process. The interdigitated electrode (IDE) structure consists of five fingers with the finger width of 600 µm, the finger length of 2900 µm and the finger spacing of 324 µm. The surface area of the IDE structure amounted 0.087 cm^{-2}. The processed wafer was diced into separate chips (chip size: 10 mm x 10 mm). The BST films of $Ba_{0.25}Sr_{0.75}TiO_3$ composition were prepared by pulsed laser deposition technique by using targets fabricated via the self-propagating high-temperature synthesis at NPUA. The process steps of the BST synthesis are described in detail in [6,20]. The BST films were deposited using a Si-shadow mask. The deposition was performed in an oxygen atmosphere (gas flow 30mL/min, pressure $2x10^{-3}$ mbar) using a KrF-excimer laser (Lambda LPX305) with a pulse width of 20ns and a pulse energy of approximately 1J per pulse. When using deposition time of 100s, energy density of 2.5J cm^{-2} and repetition rate of 10Hz, the BST layer thickness amounted approximately to 120nm.Finally, the sensor chip coated with BST was mounted on a printed circuit board, followed by ultrasonic wire bonding and encapsulation processes.

3. Experimental

Since barium (strontium) titantate (BST) ferroelectric thin films are widely used in memory devices, tunable capacitors, infrared detectors, surface acoustic wave (SAW) devices, microactuators and bio (chemical) sensors, an attempt has been made to study the effect of high energy electron beam irradiation on the electric, dielectric and ferroelectric properties of those thin films. There are only a few reports on the study of high energy electron beam irradiation effects on ferroelectric thin films.
The objectives for this work are:
a. To prepare and/or obtain BST nano-film based structures.
b. To irradiate them by different electron beam dose levels.

c. To perform electronic characterization to determine the dose vs. effect relationships for various ferroelectric property parameters.
d. To use the experimental results to draw conclusions about nature of the post-irradiation defect microstructure.
e. To perform numerical simulations and employ models to investigate the damage event at the atomic scale and, if possible, make predictions about the resulting damage microstructure and its effect on measured material property changes.

The experiments have been carried out in CANDLE at AREAL laboratory. The energy of electrons has been 4 MeV, bunch charge 10-200pC, repetition rate 1-50 Hz. The capacitance, C-*f*, dielectric permittivity, ε-*f*, and loss tangent, tgδ-*f* dependencies before and after irradiation are presented in Figures 2, 4 and 5.

3.1 C-V measurement and modeling

The results of *C–f* measurements were done at the range of frequency 100 Hz -1MHz using a computer interfaced QuadTech 1920 LCR meter (Agilent) measuring unit and High Resistance meter 4339B(Agilent) at room temperature (300 K) are presented in Fig.2.

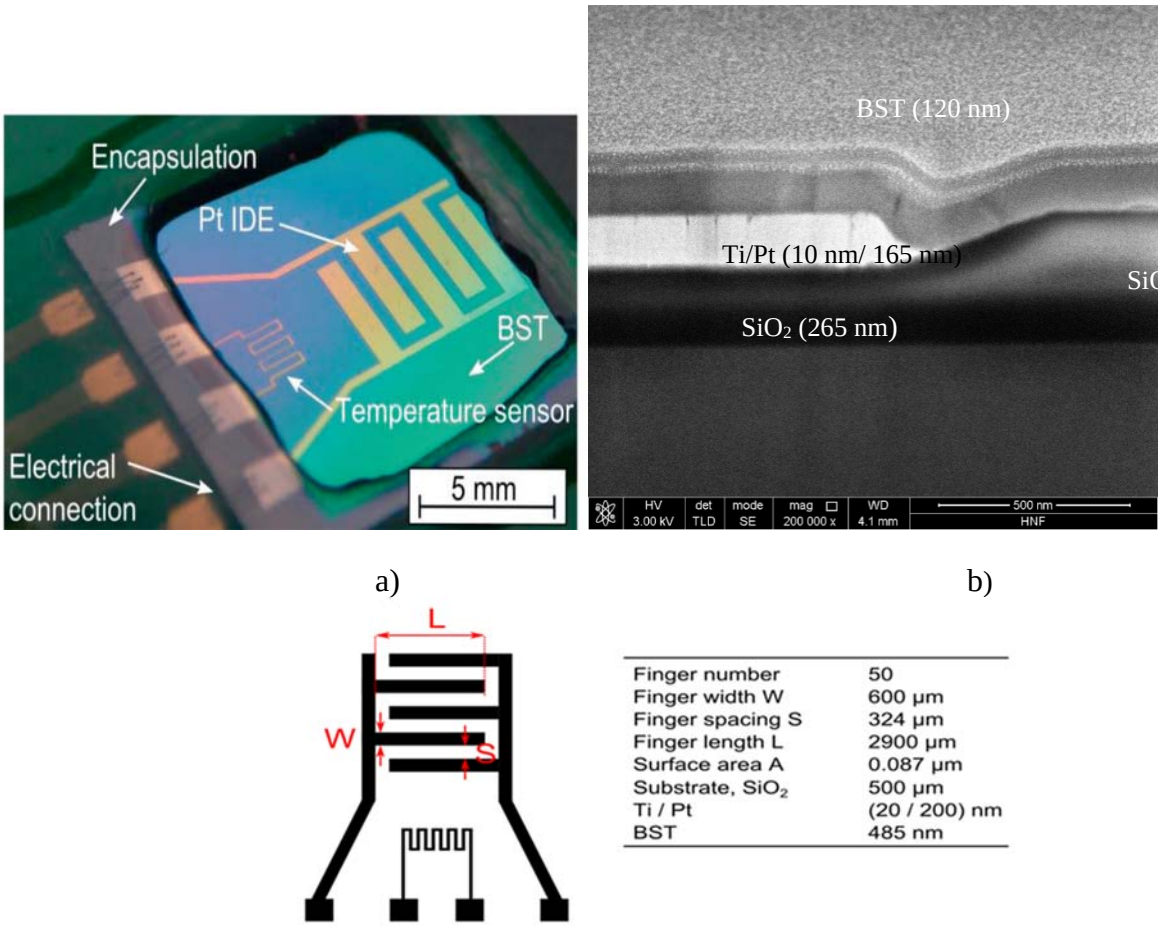

Fig. 1. Photography of a fabricated sensor chip - (a), cross-sectional SEM image showing the Si-SiO_2-Ti-Pt-BST layer stack - (b) and sizes of IDE geometry - (c)

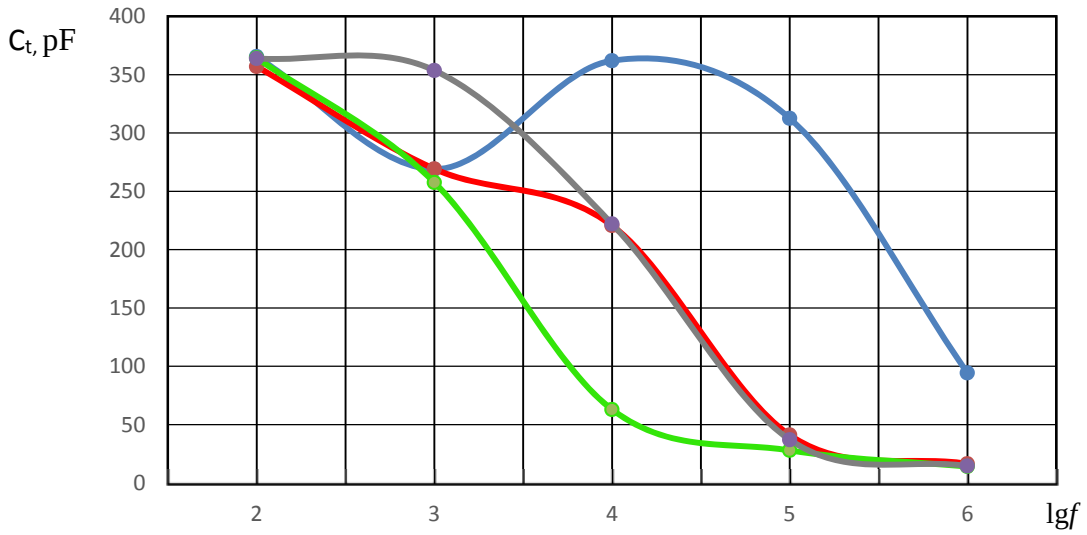

Fig.2. The C–lg*f* dependences of examined structure before (blue line) and after the irradiation (red-after the first irradiation, 27.03.2015, green- after the second irradiation, 07.04.2015, and purple after the third irradiation, 14.04.2015)

As it follows from Fig.2, in general, irradiation leads to shift of *C–f* curves to the more low frequency range and tends to decrease of capacitance at the same conditions, which in turn, indicated to decrease of dielectric permittivity. This kind of change has been observed from other authors for BST films [18] and PZT capacitances too [22,23].

For calculation (evaluation) of values of ferroelectric thin film dielectric permittivity, ε_f, we used the results, obtained in [24-26], developed for multilayer planar interdigitated electrodes capacitance (IDC) which, in turn, based on conformal transformation method [27].

For ε_f calculations we have used the following expressions of IDC.

$$C_{t_o t} = (n-1) l \cdot C_1,$$

where $C_{t_o t}$ is the total (measured) capacitance of the structure, n is the amount of fingers, l is the length of the fingers,

$$C_1 = \frac{\varepsilon_o \varepsilon_f}{2} \cdot \frac{K[(1-k^2)^{1/2}]}{K(k)} = \frac{\varepsilon_o \varepsilon_f K(k^1)}{2 \cdot K(k)},$$

$K(k)$ is the complete elliptic integral of the fins t kind with modules of k.

For more than two fingers the periodicity of the structure allows to determine k as:

$$k = \cos\left(\frac{\pi}{2} \cdot \frac{w}{w+S}\right),$$

where w is the width of the finger, S is the space between the fingers.

According to Fig.3, where presented the equivalent circuit of structure

$$C_{t_o t} = C_s + C_\beta + C_f + C_{exp} + C_i,$$

where C_s is the capacitance of the substrate (pS_i), C_β is the parasitic capacitance between P_t eletrodes (fingers), C_f is the capacitance of ferroelectric film, C_{exp} is the capacitance of the measurement set-up, C_i is the insulator lager (SiO_2) capacitance.

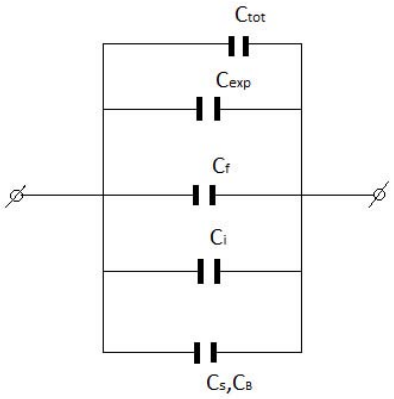

Fig.3.Equivalent circuit of examined structure

The numerical calculations of C_i, C_β show, that their values about two order less than that for C_f and ignoring also the C_s , C_β and C_{exp}, we used the approximation of:

$$C_{tot} \cong C_f \cong C_{measure},$$

Finally, for the calculation of ε_f we have used:

$$\varepsilon_f \cong \frac{2C_{tot}}{\varepsilon_o \cdot l \cdot (n-1)} \cdot \frac{K(k)}{K(k^1)} .$$

The *extracted* (evaluated) ε-*f* dependences before and after irradiation are shown in the Fig.4.

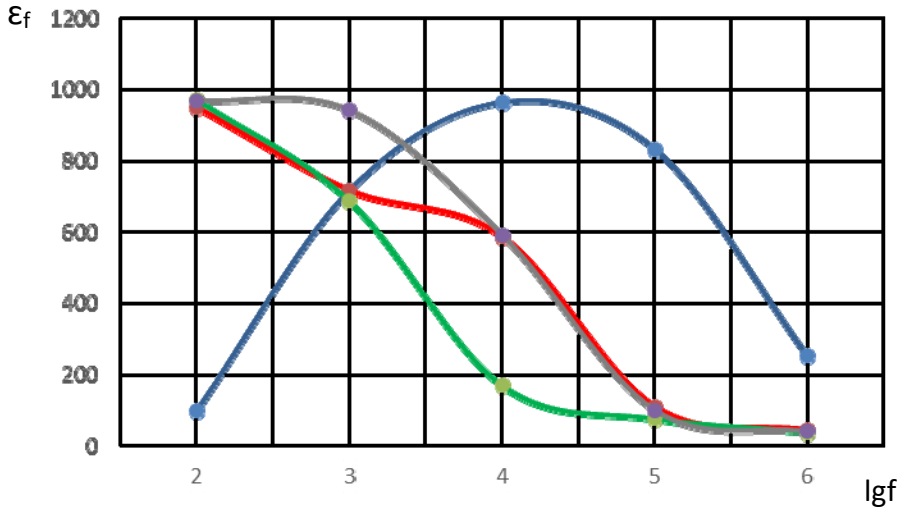

Fig.4.The ε-lgf dependences of examined structure before (blue line) and after the irradiation (red-after the first irradiation,27.03.2015, green- after the second irradiation, 07.04.2015, and purple after the third irradiation, 14.04.2015)

As it follows from Fig.4, the dielectric permittivity, in general, after the all irradiations tends to shift to the more low frequency range and after the first and second irradiation is decreased, but at least, after the third irradiation it tends to relax remaining in the low frequency ranges. This change can be explained by radiation induced heating influence phenomenon on dielectric constant when following the Curie-Weiss law in paraelectric regime.

3.2. Dielectric characteristics (losses)

As it is well known [24-26], there are two major groups of microwave losses in paraelectric phase ferroelectric: intrinsic and extrinsic. In ideal (perfect) single crystal paraelectric, the dissipation (losses) of the microwave power is associated with the absorption of the (microwave) electromagnetic wave by the thermal oscillations of the ions, and by the free charge carriers. These intrinsic losses are typically small and not be eliminated or reduced. In real crystals, and especially in thin films, the dissipation of the microwave energy is associated with the defects and may be much higher. On the other hand, as free charge carriers density and its mobility in ferroelectrics usually are small the losses associated with the absorption of the electromagnetic energy by the free charge carriers may be ignored in most of cases (because the losses are additive, i.e. the total loss tangent of a paraelectric crystals is a sum of the loss tangents of all involved mechanisms). It means that the fundamental loss sources connected with the interactions of electromagnetic energy with the thermal oscillations (phonons) of the ions and due to absorbed energy by thermal phonons, the dissipated energy heats the crystal. As the energy of phonons in the crystal is much higher than the quantum *hf* of the microwave field, hv>*hf* (*h* is the Plank's constant, v is the oscillation frequency, *f* is the frequency of microwave field) in terms of quantum mechanics the absorption takes place via three and four quantum mechanisms [24-26].In microwave and millimeter wave and near room temperature regions this theory predicts the following frequency dependence on temperature:

$$\tan\delta_{ph} \propto \omega\varepsilon^{3/2}T^{2}.$$

Here, δ is the angular frequency and ε is the relative permittivity of ferroelectric, T is the absolute temperature.

In real crystals and thin films besides the fundamental phonon losses extra losses can be appear due to free charge carriers and under the external electric field. The external fields, both DC, and even high power microwave fields can break the symmetry of the crystal structure and induced non-center symmetric unit cell of the crystal lattice becomes polarized with the external field dependent dipole moment. In an extreme case, the external DC field may cause paraelectric to ferroelectric phase transformation, resulting in a rapid increase of microwave losses. The extrinsic microwave loss mechanisms in the ferroelectrics are summarized by Vendik [24] and Tagantsev [25]: (i) loss owing to charged defects, (ii) universal relaxation law mechanism, (iii) quasi-Debye contribution induced by random-field defects. The induced electric dipole initiates two extra mechanisms of the losses: i) DC field induced Quasi-Debye, and ii) microwave to acoustic transformations. The i) mechanism, proposed by Tagantsev [25] for small tuneability, the losses associated with this mechanism are characterized by the following functional dependences of the loss tangent on the frequency and electric field:

$$tan\delta_{QD} = AI(E)\omega T(E),$$

where T(E) $=\frac{\varepsilon(0)-\varepsilon(E)}{\varepsilon(0)}$ is the tuneability, $I(E)$~1, A is the material related constant (for STO, experimental values of A~ $23\cdot10^{-3}$/GHz), $\varepsilon(0)$and $\varepsilon(E)$ are the permittivity at zero and E field, respectively.

For a small tunability, T(E)<< 1, using the non-linear dependence of ferroelectrics on DC field, $\tan\delta_{QD}$ can be presented as:

$$tan\delta_{QD}=3A\beta[\varepsilon(0)/\varepsilon(E)]^3\omega E^2,$$

where β is the coefficient of the dielectric nonlinearity (for STO, for example, $\beta=6.53\cdot10^{-4}$ [2, 24,25]).

It is necessary to note that especially in thin films, all intrinsic losses are "screened" by higher contributions from extrinsic losses, which are associated with the defects. Charged point defects (mainly oxygen vacancies [28] seem to be the most common positively charged defects in ferroelectrics) and charged dislocations create local static electric field which locally distort the crystal symmetry and create local dipole. In such local field, both electrostrictive and converse piezoelectric effects are active and the electromagnetic (microwave) wave generates acoustic waves that move in the crystal taking with them some energy from microwaves, i.e. causing loss of the microwave signal. The loss tangent associated with the charged defects is approximated by [1,2,24-26]:

$$\tan\delta_{ch}=F\varepsilon\omega\frac{Z^2n}{4\pi\rho v_t^3}\left\{1-\frac{1}{\left[1+\left(\omega/\omega_c\right)^2\right]^2}\right\},$$

where F~1is the material specific constant, Z is the effective charge (C) of the defects, n is the density (m^{-3}) of the defects, ρ is the density of the crystal (kg/m^3), v_t is the acoustic velocity, $\omega_c=v_t/r_c$, r_c is the correlation length of the charge distribution, i.e. distance at which the electro-neutrality in the crystal is restored.

As it follows from $\tan\delta_{ch}$ expression, the loss tangent in this case is proportional to the permittivity, indicated the same temperature and field dependences. For a paraelectric this means a reduction of the losses with increased field and temperature. Other sources of extrinsic losses connected with the polar regions at the interfaces between the phases, grains, columns, electrodes and other layers (i.e. dielectric and metallic buffer layers). No reports are available on the losses associated with these defects. In paraelectric phase defect-less single crystals and low temperatures, the quasi-Debye mechanism dominates. It is characterized by linear frequency dependence and a field dependence which at low field strengths may be approximated by a quadratics function. However, the experiments reported until now indicate that losses in the thin films increase linearly with the frequency and decrease with the electric field, i.e. it seems the losses associated with the charged defects dominate.

The loss tangent, tanδ, for non-irradiated and irradiated BST thin films measured at room temperature as a function of frequency is shown in Fig.5.As it follows from the Fig.5, the loss tangent, tanδ, due to irradiation tends to shift to the more low frequency range and, after the first and second irradiation, the tanδ is decreased, but at least, after the third irradiation it tends to relax remaining in the low frequency range. For all cases, tanδ increases with increasing of frequency and for the non- irradiated ferroelectric film can be approximated by a quadratics function. This means that the quasi-Debye mechanism dominated. After the first irradiation the loss tangent is in linear dependence on frequency and then after the second and third irradiations it has linear-quadratic dependence which indicated that with the quasi-Debye mechanism the charge defects mechanism plays any role too. This kind of dependence are in accordance of above mentioned mechanism originated for ferroelectrics, i.e. losses in the thin

films increase linearly with the frequency and it seems the losses associated with the charged defects dominate. This kind of change can be associated with the radiation-induced oxygen vacancies which are the main type of defect produced by electron irradiation. To reveal this prediction, more accurate and new experiments are needed.

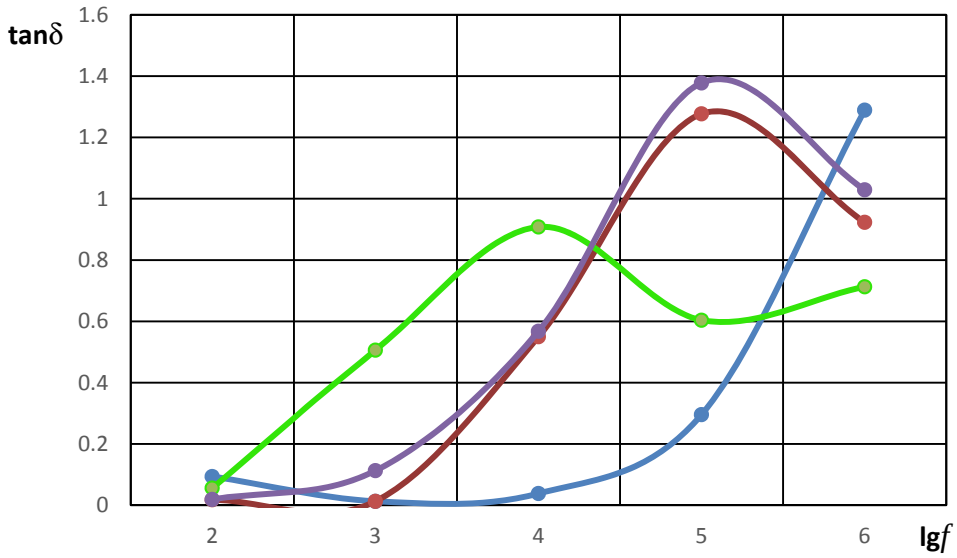

Fig.5. The tanδ -lgf dependences of examined structure before (blue line) and after the irradiations (red-after the first irradiation, 27.03.2015, green- after the second irradiation, 07.04.2015 and purple - after the third irradiation,14.04.2015)

Acknowledgment

The authors are grateful to Prof. M. Schoening, Prof. A. Poghossian and Dr. C. Huckfrom Aachen University of Applied Sciences, Institute of Nano- and Biotechnologies, Campus Juleich, Germany, for their support during the preparation of samples. This work was supported by State Committee of Science MES RA, in frame of the research project № SCS 14AR-2f12.

References

[1] M. Dawber, J.F. Raba, J.F.Scott. Physics of thin-film ferroelectric oxides. Rev. of Modern Phys., v.77, pp.1083-1130, 2005.

[2] S.Sh. Gevorgian, A.K. Tagantsev, A. K. Vorobiev. Tunable Film Bulk Acoustic Wave Resonators. Springer-Verlag, London, 2013, 243p.

[3] A.K.Tagantsev, V.O.Sherman, K.F. Astafiev, et al. Ferroelectric Materials for Microwave Tunable applications. J. of Electroceramics, pp.11-66, 2003.

[4] H.Ishiwara, M.Okuyama, and Arimoto Y. (Eds,). Ferroelectric random access memories// Fundamentals and applications, Topics in applied physics. v. 93, Publisher: Springer-Verlag Berlin and Heidelberg GmbH & Co. KG. 2004.

[5] C.-Y. Chen, J.-C. Chou, H.-T. J. Chou.pH sensing of $Ba_{0,7}Sr_{0,3}TiO_3/SiO_2$ film for metal-oxide-semiconductor and ion-sensitive field-effect transistor devices. Journal of the Electrochemical.Society 156, N6, p.p. G59-G64. 2009.

[6] V.V. Buniatyan, M.H. Abouzar, N.W. Martirosyan, et al. pH-sensitive properties of barium strontium titanate (BST) thin films prepared by pulsed laser deposition technique. Physica Status Solidi A 207, pp.824-830, 2010.

[7] C. Huck, A. Poghossian, M. Bäcker, et al. Multi-parameter sensing using high-*k* oxide of barium strontium titanate. Phys. Status Solidi A 212, N6, pp.1254-1250,2015.

[8] Q.N. Pham, C. Bohnke, J. Emery, et al. A new perovskite phase LiCaTaO: Li ion conductivity and use as pH sensor. Solid State Ionics 176, pp. 495-504, 2005.

[9] M. Roffat, O. Noel, O. Soppera, et al. Investigation of the perovskite ceramic $Li_{0,30}La_{0,56}TiO_3$by pulsed force mode AFM for pH sensor application. Sensors and Actuators B: Chemical 138, pp.193-200,2009.
[10] G. Wang, Y. Bao, Y. Tian, et al. Electrocatalytic activity of perovskite $La_{1-x}Sr_xMnO_3$ towards hydrogen perovskite reduction in alkaline medium. Journal of Power Sources 195, pp.6463-6467, 2010.
[11] G.L. Luque, N.F. Ferreyra, A. G. Leyva, et al. Characterization of carbon paste electrodes modified with manganese based perovskites-type oxides from the amperometric determination of hydrogen peroxide. Sensors and Actuators B: Chemical 142, pp. 331-336, 2009.
[12] K. Sahner, R. Moos. Modeling of hydrocarbon sensors based on p-type semiconducting perovskites. Physical Chemistry Chemical Physics 9, pp.635-642, 2007.
[13] S. Agarwal, G.L. Sharma. Humidity sensing properties (Ba, Sr)TiO_3thin films grown by hydrothermal-electrochemical method. Sensors and Actuators B:Chemical 85, pp.205-211,2002.
[14] W. Zhu, O.K. Tan, Q. Yan, et al. Microstructure and hydrogen gas sensitivity of amorphous (Ba, Sr)TiO_3thinfilm sensors. Sensors and Actuators B: Chemical 65, N1-3, pp. 366-370, 2000.
[15] S.C. Roy, G.L. Sharma, M.C. Bhatnagar, et al. Novel ammonia-sensing phenomena in sol-gel derived $Ba_{0,5}Sr_{0,5}TiO_3$thin films: Sensors and Actuators B: Chemical 110, N2, pp.299-302,2005.
[16] Ф.Коршунов, Г.Гатальский, Г.Иванов. Радиационные еффекты в полупроводниковых приборах. Минск, Изд.”Наука и техника”, 1978,230с.
[17] S. Aparna, V. M. Jali, G. Sanjeev, et al. Dielectric properties of electron irradiated PbZrO3 thin films. Bull. Mater. Sci., v. 33, No. 3, pp. 191–196, 2010.
[18] V.A.Balakin, A.I.Dedik, S.F.Karmanenko et al. The influence if electron beam on dielectric properties of ferroelectric BSTO films, Pisma JTF, v.29, pp.77-83, 2003.
[19] H. N. Yeritsyan1, A.A. Sahakyan1, N. E. Grigoryan1, et al. Clusters of Radiation Defects in Silicon Crystals, Journal of Modern Physics, v. 6, pp. 1270-1276, 2015.
[20] C.Huck, A. Poghossian, M. Backer, et al. Capacitively coupled electrolyte-conductivity sensor based on high-k material of barium strontium titanate. Sensors and Actuators B: Chemical, v. 198, pp. 102–109, 2014.
[21] C. Huck, A. Poghossian, M. Bäcker, et al. Multi-parameter sensing using high-*k* oxide of barium strontium titanate. Phys. Status Solidi *A212*, N6, pp.1254-1250,2015.
[22] J.-L. Leray, O.Musseau, P. Paillet et al. Radiation effects in Thin-film ferroelectric PZT for Non-Voltailememory Applications in Microelectronics. J. Phys III France, v.7., pp.1227-1243, 1997.
[23] C.M. Othon, S. Ducharme. Electron Irradiation Effects on ferroelectric Copolymer Langmuir-Blodgett films. Ferroelectrics, 304, pp.9-12, 2004.
[24] O.G. Vendik, I.T. Ter-Martirosyan and S,P, Zubko.Microwave losses in incipient ferroelectrics as function of the temperature and the biasing field. J, Appl. Phys., v,84, pp.993-998,1998.
[25] A.K. Tagantsev, V.O. Sherman, K.F. Astafiev et al. Ferroelectric materials for microwave tunable applications, J. Electroceramics., v.11, pp. 5-66, 2003.
[26] S.Sh..Gevorgian. Ferroelectrics in Microwave Devices, Circuits and Systems. *Springer-Verlag, London*, 2009, 394p.
[27] A. Nussbaum, Electromagnetic theory for engineers and scientists, Prentice –Hall, Englewood Cliffs, 1965, 464p.
[28] V.V. Buniatyan, N.W. Martirosyan, A.K. Vorobiev, et al..Dielectric model of point charge defects in insulating paraelectricperovskites. Journal of Applied Physics, 110, pp. 094110-1-11, 2011.